
Article:
Aende, A, Gardy, J orcid.org/0000-0003-1806-4056, Aslam, Z et al. (5 more authors) (2022) A novel highly osmotic K/Fe_3O_4/CNF magnetic draw solution for salty water desalination. Desalination, 538. 115903. ISSN 0011-9164

https://doi.org/10.1016/j.desal.2022.115903

Graphical abstract:

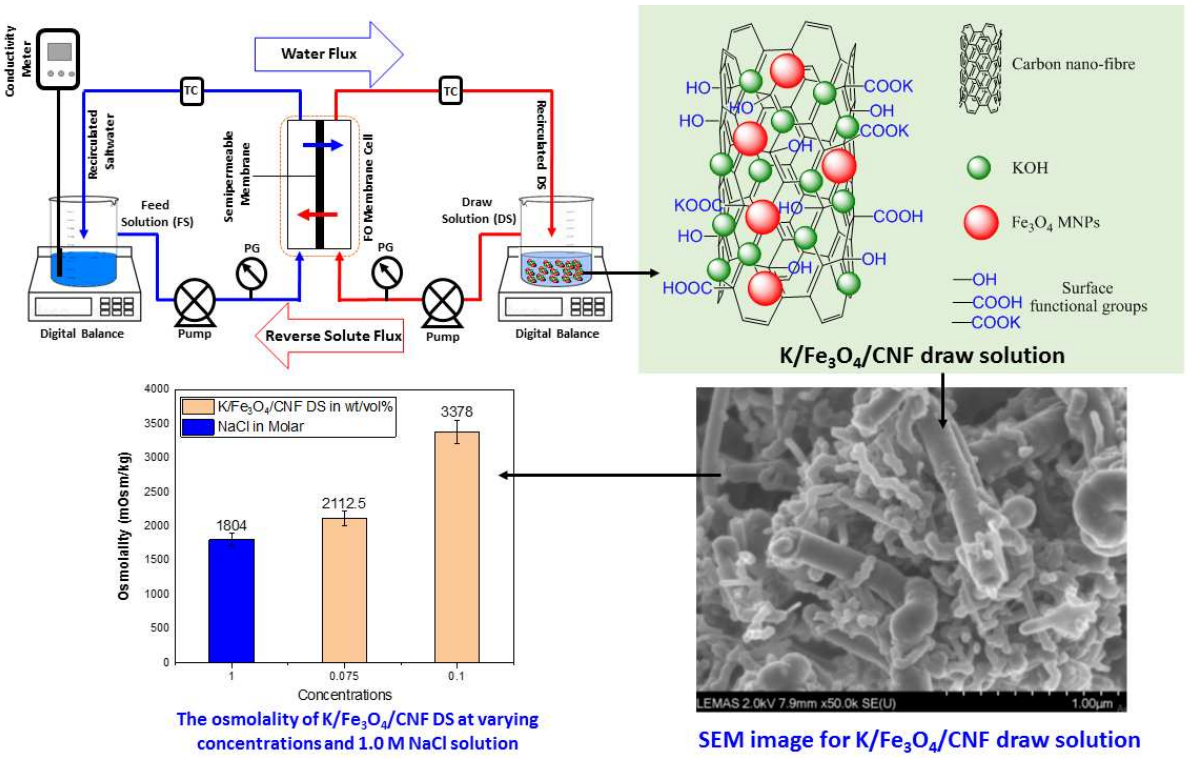

Highlights:

- MNP DS appraisal against high salinity feed streams is more rational.
- The DS preparation protocol enhanced MNP hydrophilicity without polymers.
- K/Fe_3O_4/CNF DS produced high osmotic pressure (86.1 bar) and water flux (24 LMH).
- K-species considerably improved the DS hydrophilicity.
- DS material feasibly recoverable via magnetic field and solar-thermal separability.

A novel highly osmotic K/Fe_3O_4/CNF magnetic draw solution for salty water desalination

Aondohemba Aende[a], Jabbar Gardy[a,*], Zabeada Aslam[a], Matthew Rogers[b], Mohamed Edokali[a], Oscar Cespedes[b], David Harbottle[a], Ali Hassanpour[a,*]

[a]School of Chemical and Process Engineering, Faculty of Engineering and Physical Sciences, University of Leeds, Leeds, West Yorkshire, Leeds, LS2 9JT, UK

[b]School of Physics and Astronomy, Faculty of Engineering and Physical Sciences, University of Leeds, Leeds, West Yorkshire, Leeds, LS2 9JT, UK

Abstract:

Forward osmosis (FO) is increasingly being studied as an alternative desalination technique to the other conventional desalination technologies, owing primarily to its low energy potential. However, the co-opted energy limitations in the draw solution (DS) regeneration stage in FO desalination processes and the lack of effective DS have hampered FO's implementation for potable water application on an industrial scale. In this work, we explored the Donnan principle to engineer a DS material having the duality of magnetic and solar-thermal separability functionalities from a sustainability viewpoint whilst exploiting a careful selection of material properties. A novel potassium functionalised iron oxide doped carbon nanofibres (K/Fe_3O_4/CNF) magnetic nanoparticles (MNPs) was successfully synthesised for FO desalination applications, utilising an eco-friendly strategy that improves hydrophilicity of DS without polymers. The novel DS obtained a significant osmotic pressure (86.1 bar), while it FO performance showed a small reverse salt flux (RSF) and specific reverse salt flux (SRSF) values of 0.56 gMH and 0.02 g/L, respectively. These values compare to at least less than 10% of most RSF and SRSF values reported in the literature. The facile DS synthesis strategy adopted herein will potentially open a new route to preparing other DS nanomaterials with unique multi functionalities and enhanced hydrophilicity devoid of polymers. Whilst magnetic DS re-concentration may be achievable, additional research is required to appraise this

methodology's overall energy implications and economic advantages over existing DS recovery methods.

Keywords: Water desalination; Forward osmosis; Magnetic nanoparticles: Draw solutions; Osmotic pressure; Carbon nanofibres.

1. Introduction

In response to addressing the global challenge of freshwater insecurity, desalination of saltwater as a means of increasing global freshwater supplies via technology has been advanced amongst other solutions due to the preponderance of saltwater on the earth's surface [1]. Notable technologies, including multi-stage filtration (MSF), multi-effects distillation (MED), vapour compression (VP), reverse osmosis (RO), electrodialysis, etc., have been exploited [2, 3]. However, it is mostly held that desalination as a practice is energy-intensive [4]. Forward osmosis (FO), a natural process, has gained tremendous research interest in recent years as an alternative desalination technique [2]. This is because the FO process is often considered as having a low fouling propensity relative to pressurised membrane processes like reverse osmosis (RO), good salt rejection ability, and, more importantly, its supposedly low energy potentialities [2, 5]. The FO process is propelled by the concentration gradient (osmotic pressure difference) across a semipermeable membrane between two solutions. As an emerging desalination technique, FO has demonstrated some tried-and-true abilities to desalinate saltwater [5] and is deployable in treating highly vitiated source waters [6, 7]. However, FO's supposedly low energy potentials as a desalination technique are seriously challenged during DS recovery and regeneration. The energy involved at this stage often exceeds the minimum thermodynamic energy of separation for seawater (1.56 kWh/m^3) at 50% recovery [8]. This is because more than one process or a secondary technique (s) is required at the DS regeneration stage to obtain pure water successfully. At this point, any attendant energy deficiencies of these

secondary techniques get arrogated to the overall FO process. Over the years, different categories of DS materials, including organic salts, inorganic salts, volatile compounds, stimuli-responsive materials, polyelectrolytes, and carbon-based materials, have been exploited across various research studies for potential application in FO desalination systems [9]. However, most of these materials, such as organic and inorganic salts, volatile compounds, and polyelectrolytes, suffer from severe reverse salt flux, occasioning concentration polarisation (CP) effects. [2] Consequently, the osmotic pressure difference across the membrane and, by extension, water flux is negatively influenced. The potential cost implication of replenishing the lost DS materials is considered expensive [2, 9]. Furthermore, the requirement of membrane-based downstream processes such as RO, membrane distillation (MD), nanofiltration (NF), and ultrafiltration (UF) to achieve DS re-concentration adversely impacts the FO system's energy efficiency, which is a downside [2]. On the other hand, low water recovery rates associated with stimuli-responsive DS materials render them unsuitable for industrial applications. Therefore, recent research efforts to engineer new and improved DS materials, particularly those that mitigate the energy limitation imposed during the DS recovery stage in FO desalination systems, led to considering the application of MNPs as DS materials [9]. Magnetic separation involving a magnetic field is gaining considerable research attention as a potentially viable DS regeneration mechanism that could address the energy deficiencies in FO desalination imposed by the secondary recovery processes [9]. This is primarily due to the potentially low energy and convenience of applying this methodology, particularly the ability of MNPs to be separated by low-cost magnets [10, 11]. Nanoparticles (NPs) of iron oxide preponderate studies for applications as MNPs DS in FO desalination research studies [9]. Principal amongst the increased focus on iron oxides MNPs as DS is their chemical stability, biological compatibility, insignificant toxicity, and the fabrication of Fe_3O_4 and Fe_2O_3 into NPs facilely [12]. Several studies have fabricated a host of surface functionalised MNPs

with polymers as draw agents for applications in FO systems [11, 13-20]. However, despite some appreciation in the study of MNPs as DS, particularly in desalination research, a key challenge remains the somewhat inability of most of these materials to develop considerable osmotic pressure enough to facilitate water transfer across a semipermeable membrane. For example, Ling et al. [21] studied a FO system combining a low-intensity magnetic field to facilitate magnetic separation of DS and mitigate agglomeration, The poly(N-isopropyl acrylamide) and tri-ethylene glycol functionalised MNPs (PNIPAM/TRI) as the representative DS in this study generated a very low water flux (< 2LMH) after five cycles which is a downside. Moreover, the DS fabrication methodology is seemingly complicated, which can constitute cost increases [9]. Additionally, according to research, magnetic fields are not always able to entirely capture MNPs, particularly those of decreasing particle sizes [22]. As a result, ultrafiltration is considered a suitable post-treatment to concentrate MNPs draw solutes because its pore size may be small enough to capture MNPs without the attendant effects presumably of using NF and RO, the commonly utilised techniques to intercept salts and organic chemicals [23]. However, based on research in the literature, it is established that regardless of any DS type and any pressure-driven recovery technique employed, the energy consumption of any such hybrid FO system is effectively indistinguishable from any other [24]. In addition, another investigation revealed that MNPs of smaller sizes than a UF membrane pores uncaptured by a magnetic field reconcentration could permeate through the membrane [25]. This can pose a hindrance to industrial application due to potential health implications, thus necessitating further research to optimise this deficiency. Concentrating the uncaptured MNPs via solar-thermal evaporation will offer sustainability. Furthermore, whilst polymer compounds confer the needed hydrophilicity in MNPs, some polymers can be hazardous in water, even in trace amounts [9]. Consequently, the complicacy of separating these polymers from water often using processes like RO undermines the FO's main beneficence. Therefore, from an

environmental sustainability point of view it will be well-thought to explore sustainable means of inducing hydrophilicity in MNPs [26]. Many investigations using MNPs as DS in FO desalination use DI water as the FS [11, 13-20] There is insufficient research on MNPs DS against saline FS since few studies use FS in saltwater environments [15, 26-28], thus, creating a gap in understanding how these materials operate in veritable saltwater settings. Testing these materials' osmotic action in saltwater conditions would be more well-advised.

Therefore, this work aims to feasibly explore, from a sustainability viewpoint, approaches that can facilitate the enhanced application of MNPs as DS in effectuating the FO process. To meet our objective, we attempt to exploit the tenets of the Donnan mechanism to synthesise engineered DS materials with dual functionality of magnetic and solar-thermal separability/re-concentration to facilitate improved membrane water flux. Specifically, the work will: (i) exploit a blend of unique material properties for draw solutes fabrication to foster high osmotic pressure, improved water flux and facilitate DS re-concentration via a magnetic field and solar irradiation (ii) conduct the material characterisation and osmotic performance evaluation of the as-fabricated draw solutes relative to modelled saltwater solution as feed. The performance would be examined relative to parameters including osmotic pressure, water flux, reverse salt flux, and specific reverse salt flux. Therefore, this work presents a novel K/Fe_3O_4/CNF MNPs as DS for application in FO desalination operations. The novel DS not only exhibits high osmolality and, by extension, high osmotic pressure that can be tested against feed streams with high salinity but is also feasibly recoverable via a magnetic field and solar energy.

2. Materials and methods

2.1. Design strategy and material consideration

The strategy is to exploit a unique blend of material properties to effectuate the Donnan effect in the FO process in anticipation that when in aqueous media, the DS material will generate

146 significant charges to repel the NaCl ions' activity around the membrane's active layer.
147 Consequently, this will allow water as the primary eluent in the FS to permeate with ease,
148 increasing the membrane water flux. We premised the material choice on the following
149 consideration:

150 1. Carbon in CNF, because of its outstanding solar-thermal properties coupled with its
151 unique physicochemical properties, allows it to be multi-functionalized by covalent or
152 non-covalent modifications or a combination to achieve multiple vital functionalities.
153 2. The strong hydrophilic disposition of KOH, the excellent water solubility offered by
154 the high hydration energy of the K^+ ions, and the ability of K species to reversibly
155 intercalate
156 3. Along with its strong magnetism compared to other MNPs, iron oxide MNPs offer a
157 high reactive surface that readily fosters modification with biocompatible coatings. In
158 addition, it can be controlled and easily separated by a magnetic field for further and
159 subsequent applicable reuse.

160 Other advantages, including low cytotoxicity, natural abundance, and low cost, contribute to
161 our choice of these materials.

162

163 **2.1. Synthesis of iron oxide (Fe_3O_4) nanoparticles**

164 Fe_3O_4 NPs were synthesised via the co-precipitation method [29] as can be seen in the reaction
165 below:

166 $$Fe^{2+} + 2Fe^{3+} + OH^- \rightarrow Fe_3O_4 + 4H_2O$$

167 Briefly, an ultrasonic probe was used to separately disperse 0.2 mol of $FeCl_2.4H_2O$ (≥99.99%,
168 Sigma-Aldrich) and 0.68 mol of $FeCl_3.6H_2O$ (≥98%, Sigma-Aldrich) in a 25 mL of a 1:1 vol%
169 ethanol (Sigma-Aldrich) to deionised water solution. The obtained clear resultant solutions
170 were then transferred into a 250 mL round-bottomed flask and subsequently subjected to

171 heating at 80 ºC under the flow of N_2 atmosphere and continuous stirring (250 rpm) for 6 h.
172 Whilst the reaction mixture was under heating, 10 mL of ammonia solution (28-30 vol%,
173 NH_4OH, Sigma Aldrich) was simultaneously added dropwise to maintain the pH of the
174 solutions mixture at 12. The formed iron oxide NPs were then aged for 24 h at room
175 temperature before being isolated utilising an external magnetic field. The as-obtained NPs
176 (dark reddish particles) were then washed several times with 1:1 vol% aqueous ethanol solution
177 until no traces of chloride ions were detected using $AgNO_3$ solution as an indicator. The
178 prepared magnetic NPs were then oven-dried overnight at 120 ºC and calcined at 550 ºC for 3
179 h to obtain Fe_3O_4 MNPs.
180
181 **2.2. Synthesis of K/Fe_3O_4/CNF MNPs**
182 An 80 mL aqueous solution of a molar ratio of 1:3 of nitric acid (HNO_3) to sulfuric acid
183 (H_2SO_4) was carefully transferred into a round bottom flask. 5 g of carbon nano-fibres (CNF)
184 powder [graphitised (iron-free) compressed of conical platelets, Aldrich Chemistry, USA] was
185 then slowly added into the acid mixture and then refluxed at 70 ºC for 6 h under continuous
186 stirring at 250 rpm. The solution mixture was then filtered and repeatedly washed with
187 deionised (DI) water and dried overnight at 80 ºC using a vacuum oven. The as-treated CNF
188 powder was then dispersed in a 50 mL aqueous solution of 0.05 M sodium dodecyl (SDS) using
189 a probe sonicator for 30 min. The dispersed Fe_3O_4 MNPs and as-treated CNF were then
190 transferred into a round-bottomed flask and put under reflux at 80 ºC for 4 h whilst stirring
191 continuously at 250 rpm. Following this, a 250 mL aqueous solution of 0.5 M KOH (Sigma-
192 Aldrich) was then slowly added dropwise into the above mixture whilst stirring continuously
193 under reflux for another 4 h. The resultant mixture is then oven-dried at 60 ºC overnight and
194 washed several times using deionised water to obtain the final product labelled as
195 K/Fe_3O_4/CNF MNPs. Consequently, 1.0 wt/vol% stock solution was then prepared from the

prepared above DS by dispersing 1.0 g of K/Fe_3O_4/CNF into 100 mL of DI water, after which 7.5 mL (0.075 wt/vol%) and 10 mL (0.1 wt/vol%) respectively from the stock solution were subsequently measured and set aside for FO performance evaluations.

3. Characterisation techniques

Analysis of the structural and crystal phase of the K/Fe_3O_4/CNF MNPs was performed using the Bruker D8 X-ray diffraction (XRD) with Cu Kα radiation (λ = 1.5418 Å). The instrument was operated and maintained at a voltage of 40 kV and an applied current of 40 mA, respectively. The sample was scanned at a 2θ angle range from 10 to 70° with step size 0.0495^o at 1 sec per step.

The elemental composition, surface morphologies and location of elements for the K/Fe_3O_4/CNF MNPs sample were examined using a cold field-emission scanning electron microscopy (Hitachi SU8230 CFE-SEM). Also utilised was a transmission electron microscopy (FEI Titan3 Themis 300) coupled with the Super-X EDX system with windowless 4-detector design and the Gatan OneView 16 Megapixel CMOS digital camera for collecting bright-field TEM images. A droplet of dispersed K/Fe_3O_4/CNF in acetone was placed over a carbon-coated copper grid for examinations using a micropipette.

A Thermo Scientific^{TM} Nicolet^{TM} iS10 Fourier transform infrared (FTIR) spectrometer using the attenuated total reflection (ATR) method was employed at room temperature to examine the functional groups present in the synthesised K/Fe_3O_4/CNF MNPs, in the range of 525 – 4000 cm^{-1} at a resolution of 4 cm^{-1}. The total output was in the percentage of transmittance.

A thermo-gravimetric analysis (TGA) instrument (Mettler Toledo, TGA/DSC-3) was used to investigate the thermal stability of the prepared K/Fe_3O_4/CNF sample. The TGA analysis was performed under a constant flow rate (50 mL/min) of nitrogen purge gas and temperature range of 30 to 900 ^oC and at a 10 ^oC/min heating rate.

221 The zeta potential of the K/Fe_3O_4/CNF MNPs was investigated using the Zetasizer (Malvern
222 Instruments, UK) to ascertain their charge stability in colloidal solutions. A 1 mL syringe was
223 used to fill an aqueous K/Fe_3O_4/CNF sample into a folded capillary cuvette (Malvern DTS
224 1070), and the cuvette was then appropriately inserted into the instrument. Consequently, the
225 device is set to run after all the appropriate measuring conditions have been imputed, whilst
226 the measurements are collected in the software window.
227 The 3250 model osmometer (Advanced Instruments, USA), which measures samples
228 osmolality based on the freezing point depression principle, was deployed to measure the
229 osmolality and, by extension, the osmotic pressure of the K/Fe_3O_4/CNF.
230 The magnetic characteristics of the K/Fe_3O_4/CNF sample powder were investigated using a
231 superconducting quantum interference device (SQUID) vibrating sample magnetometer
232 (VSM). The magnetisation (M) of the powder was measured at room temperature (300 K)
233 between -1.5 and 1.5 T.
234
235 **2.4. Forward osmosis setup**
236 A lab-scale cross-flow membrane cell filtration unit (CFO42D) purchased from Sterlitech
237 Corporation Inc, USA, having an active membrane area of 42 $cm^{2,}$ was assembled and used in
238 performing the FO experiment. The CF042D cross-flow cell unit comprises tightening screws,
239 top and bottom plates, cell top and cell bottom, sintered metal support, membrane filter, and
240 O-rings. Whilst assembling the CF042D cell unit, it was ensured that the O-rings were wet with
241 water before being firmly fitted flat into the groove on the cell bottom. Ensuring that the O-
242 rings lie flat into the grooves helps avoid damage to the O-rings and leakages that may occur
243 during system operation if the O-rings are not correctly installed.
244 The FO performance of the novel K/Fe_3O_4/CNF DS was conducted in the FO mode with the
245 dense active layer (smooth side) of the commercial FTSH2O^{TM} flat sheet CTA membrane

always placed facing the FS side and the support layer (rough side) always facing the DS side. The FS and DS flow volumes were moderated utilising two Masterflex Console Gear Pumps (Cole Palmer, USA) at a steady flow rate of 1280 mL/min. The overall schematic of the setup is shown in Fig. 1.

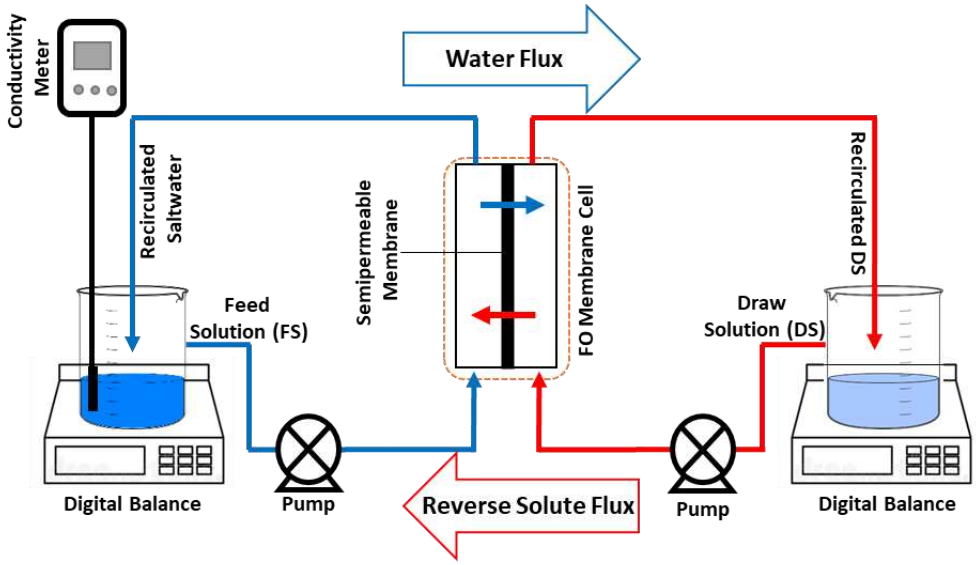

Fig. 1. The overall schematic of the FO setup.

The water fluxes across the membrane were evaluated by measuring the weight change occurring on the feed tank containing a given volume of modelled saltwater (1.0 M NaCl solution) every 5 min using an electronic balance (A&D EX300i, USA) over a 60 min period per run. Readings of the first five minutes were not considered as the system was allowed to equilibrate the flow fluctuations occasioned at the start of the experimental runs. The membrane water flux is given by:

$$J_w = \frac{\Delta m}{\rho_f A \Delta t} = \frac{\Delta V}{A \Delta t} \qquad \text{Eqn. (1)}$$

Where J_w is the permeate flux in L/m^2/h (LMH), Δm is the change in mass of the FS over time, ρ_f is the density of water, Δt is the change in time (h), ΔV is the volumetric change (L) of the FS, and A is the active membrane area (m^2) of the CTA membrane. Over the course of the FO runs, the FS's electrical conductivity (EC) measurements were obtained using a calibrated benchtop conductivity meter (VWR symphony^{TM}) every 5 min interval. The measured

conductivities (mS/cm) were then converted to concentrations [30] to evaluate reverse salt flux (RSF). The RSF was evaluated from the equation:

$$J_s = \frac{(C_t V_t - C_o V_o)}{A\Delta t} \qquad \text{Eqn. (2)}$$

Where J_s is the reverse salt flux ($g/m^2/h$), also expressed as gMH, C_o and C_t are FS concentrations at the start of the experiment and Δt respectively, V_o and V_t are the FS volumes (L) at the beginning and Δt, respectively [31].

3. Results and discussions

3.1. Characterisation of K/Fe_3O_4/CNF MNPs

The particle size of the CNF and the fabricated K/Fe_3O_4/CNF was analysed utilising dynamic light scattering (DLS). The average size of the CNF was 5.0 µm. After the doping reaction of the CNF with potassium functionalised iron (III) oxide, the average particle diameter of the K/Fe_3O_4/CNF material was 4.5 µm, demonstrating the bonding of the K species and Fe_3O_4 on the CNF.

The obtained FTIR spectra for CNF and K/Fe_3O_4/CNF samples is shown in Fig. 2 (a). The broad peak at ~3434 cm^{-1} corresponds to the O-H stretching vibrations of the -C-OH and -COOH functional groups [32, 33]. The peaks at ~2925 and ~2855 cm^{-1} correspond to the asymmetric and symmetric stretching in saturated aliphatic groups, respectively [32]. The broad peak at ~2615 cm^{-1} could be due to the O-C-O group, whilst a weak peak that followed at ~1950 cm^{-1} is related to C=C stretching vibrations [34]. A sharp peak at ~1629 cm^{-1} represents the presence of free H-O-H molecules absorbed on the sample's surface [31, 34]. Another sharp peak that follows at ~1402 cm^{-1} is related to O-H bending in carboxylic acid and alcohol [32, 34]. A weak characteristic peak at ~1106 cm^{-1} could be attributed to a C-O stretching vibration in aliphatic ether and secondary alcohols [32]. Two other bands at ~1005 and ~ 979 cm^{-1} are assigned to C-C vibrations in saturated aliphatic [32]. Subsequently, the

peak at ~830 cm^{-1} is attributed to contributions from aromatic C-H out-of-plane bending [32], whilst the absorption band at ~701, ~632, and ~558 cm^{-1} respectively could be associated with the Fe-O stretching [34]. In the case of CNF, no clear absorbed peaks were detected as the materials acted as a very effective black body absorber [35].

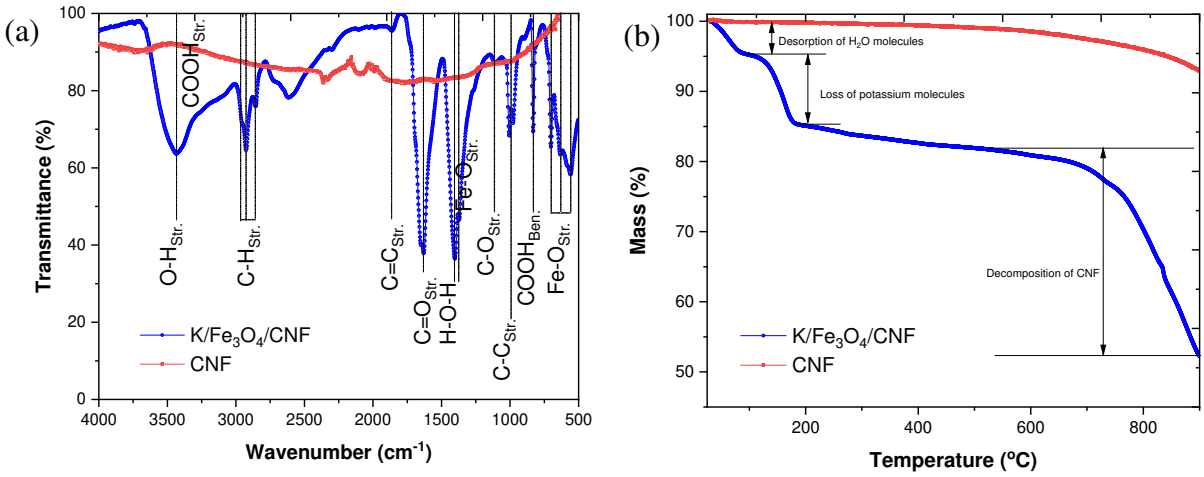

Fig. 2. (a) FTIR spectra and (b) TGA profiles for CNF and K/Fe_3O_4/CNF MNPs samples.

The thermal stability of CNF and K/Fe_3O_4/CNF MNPs samples is shown in Fig. 2 (b). There was only one stage of mass loss observed in the CNF sample, which is related to the slight decomposition of CNF at a very high temperature (started ~600 °C). However, three significant stages of mass loss are observed in the case of K/Fe_3O_4/CNF MNPs. In the first stage, an initial mass loss (~4.8 %) is noted to have occurred around 50 °C, which could be attributed to the loss of free water attached to the sample's surface. The second mass loss is observed in the temperature range of 90 to 170 °C, attributed to potassium loss. After that, no significant mass loss was noted as the sample remained relatively stable over the temperature of 170 to 540 °C. The final mass loss stage at higher temperatures spanning from 540 to 900 °C owing to the decomposition of CNF.

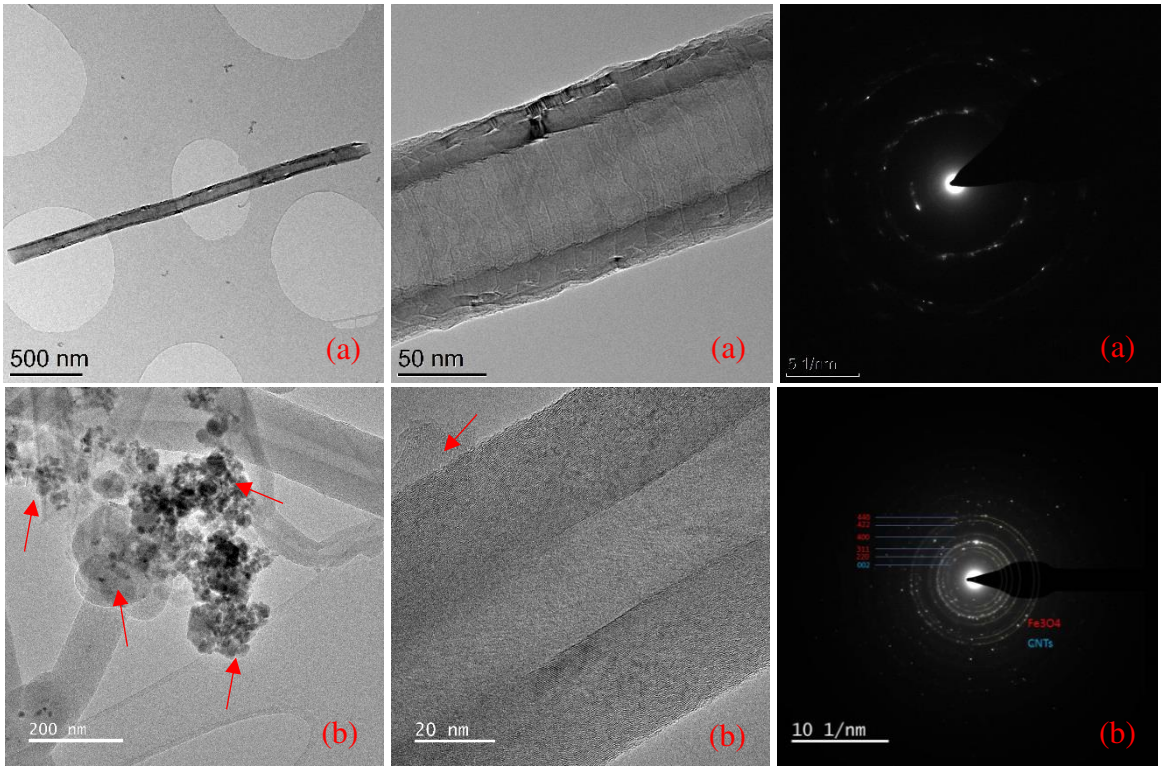

Fig. 3. TEM micrograph images and selected area electron diffraction (SAED) of the (a) CNF and (b) K/Fe_3O_4/CNF MNPs samples

Fig. 3 represents the bright-field TEM images and a selected area electron diffraction (SAED) of the CNF and K/Fe_3O_4/CNF MNPs samples at different magnifications. The SAED pattern of the K/Fe_3O_4/CNF (Fig. 3 b) shows some discrete rings corresponding to the CNF crystalline plane (002) and Fe_3O_4 crystalline planes, (220), (311), (400), (422), and (440), which identifies the CNF and Fe_3O_4 NPs in the synthesised material [36]. The TEM images for K/Fe_3O_4/CNF MNPs (Fig. 3b) show some cylindrical fibres with inwardly curved centres between some rough-like exposed edged planes. The fibres are those of the CNF, and the edge planes present sites for reactions that enable the chemical modification of the CNF surface to form composites It can also be seen from Fig. 3 (b) the formation of some rough-spherical shapes and dark spots bound on the CNF. These qualify the metal particles from the Fe_3O_4 owing to the highly ordered nature of the NPS, which gives diffraction contrasts, whilst the K-species appears matched up on the surfaces of the Fe_3O_4 and CNF in the sample. This confirms the presence of

K and Fe_3O_4 in the synthesised magnetic NPs. The presence of K-species in the sample enhances the hydrophilicity of the novel DS material, which could foster a rise in osmotic pressure [31]. In the case of CNF (Fig. 3a), the surfaces of fibres are relatively smooth and long filled cylindrical chains which can be directly related to the nature of CNF synthesis.

(a)

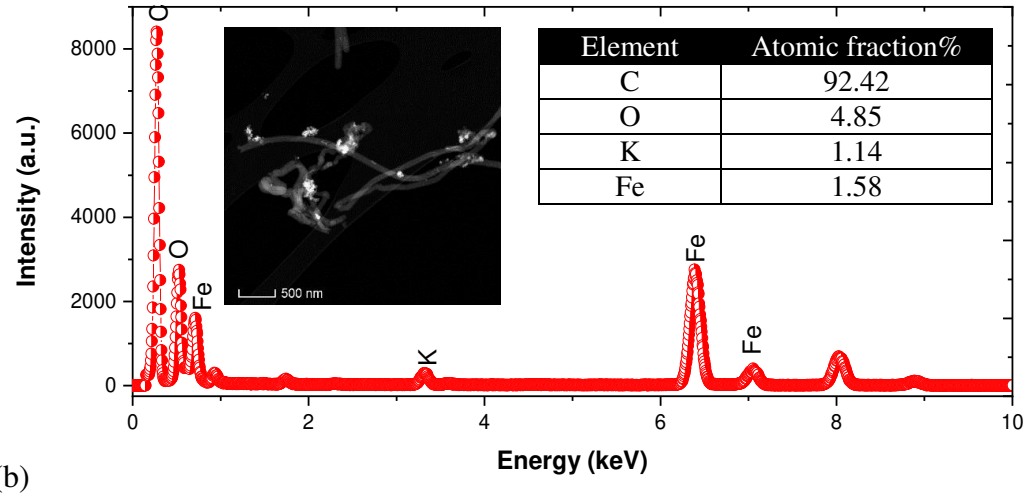

Element	Atomic fraction%
C	92.42
O	4.85
K	1.14
Fe	1.58

(b)

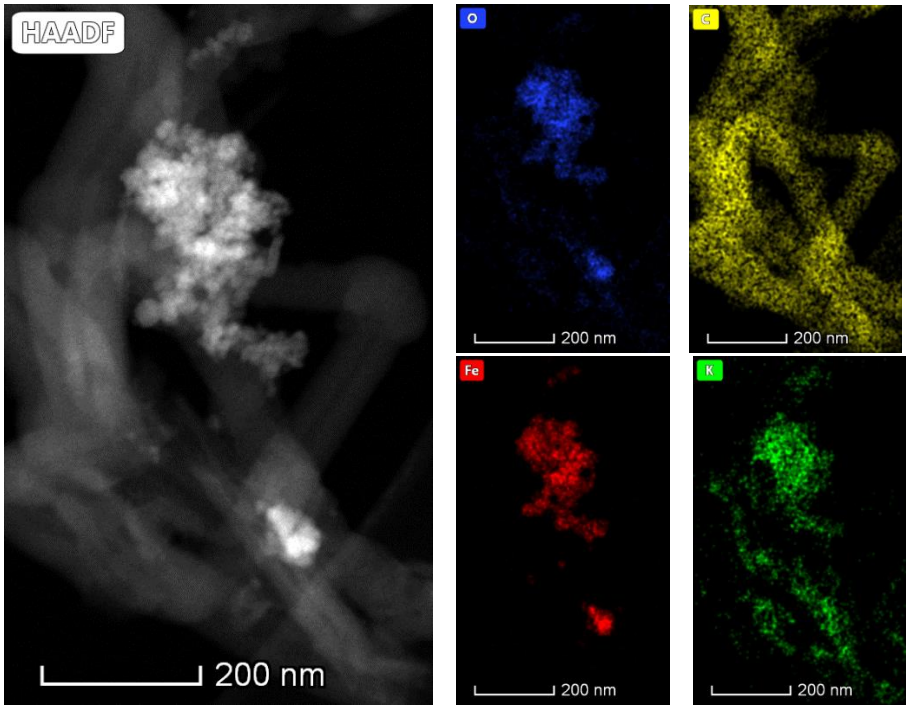

Fig. 4. (a) TEM-EDS spectrum showing the elemental composition and (b) EDS mapping of K/Fe_3O_4/CNF MNPs sample

The elemental analysis of K/Fe_3O_4/CNF MNP using EDS revealed that the synthesised sample consisted of carbon, oxygen, iron, potassium elements, as shown in Fig. 4(a). The elemental

mapping, shown in Fig. 4b), depicts clustered nanoparticles with the K-species appearing evenly distributed in the Fe NPs whilst on the other hand appearing to have overlapped with the CNF, which potentially would have modified its surface. This further confirms the successful modification of the CNF with Fe_3O_4 NPs and potassium hydroxide. The morphology of K/Fe_3O_4/CNF was further investigated using SEM analysis. Fig. 5 depicts the SEM micrographs of the K/Fe_3O_4/CNF nanocomposites at different magnifications, showing some spherical-like morphologies characteristics of Fe_3O_4 closely bounded together with some cylindrical morphologies representative of CNF.

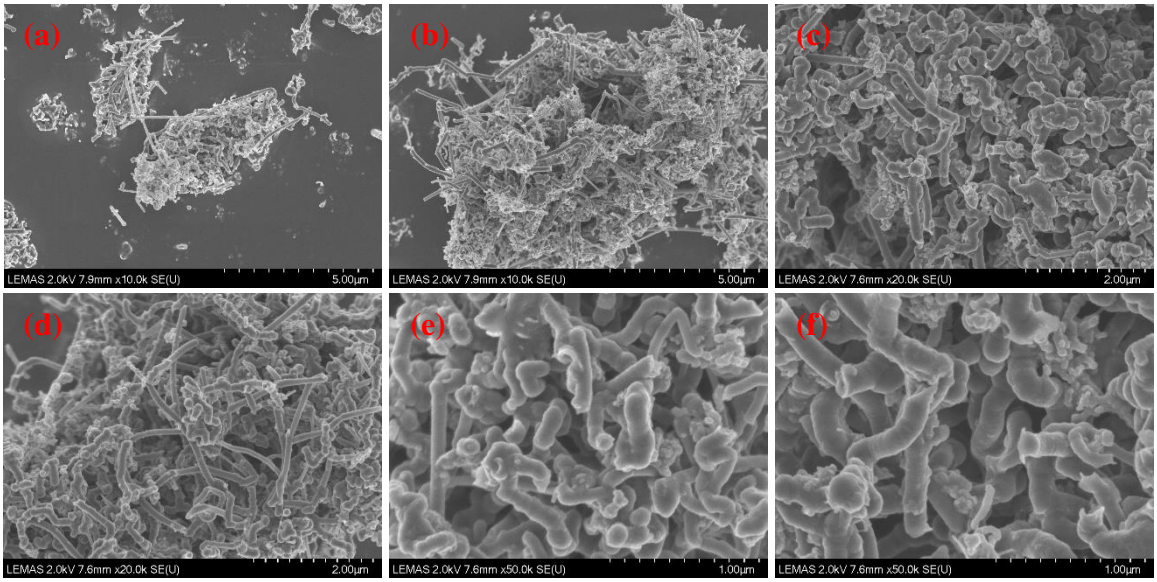

Fig. 5. SEM images for K/Fe_3O_4/CNF MNPs sample at different magnifications.

Fig. 6(a) shows the XRD profile of the K/Fe_3O_4/CNF MNPs sample. The XRD graph revealed reminiscent characteristics of the cubic spinel structure of Fe_3O_4 (JCPDS-ICDD: 04-008-8146), which often emerges in XRD patterns of Fe_3O_4 materials. The set of values of 2θ at 30°, 35°, 37°, 43°, 57°, and 62.8° are attributed to reflections at (220), (311), (222), (400), (511) and (440) planes which are common with Fe_3O_4 [37]. The other peaks could not be found in the International Centre for Diffraction Data (ICDD) database. This could result from the treatment of the CNF with strong acids and modification with KOH solution.

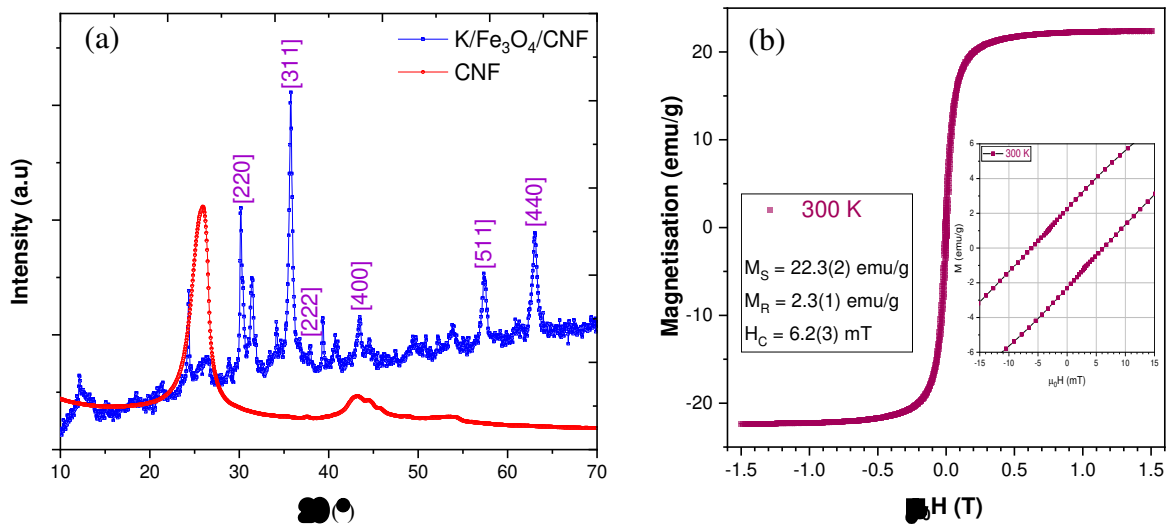

Fig. 6. (a) XRD patterns for CNF and K/Fe_3O_4/CNF samples and (b) magnetisation hysteresis loop of the K/Fe_3O_4/CNF sample at room temperature.

Fig. 6(b) shows the behaviour of the K/Fe_3O_4/CNF sample under the influence of a magnetic field at room temperature. Here, the applied field has been corrected against a palladium reference sample to mitigate the effect of trapped flux in the superconducting coil. The soft ferromagnetic behaviour required to separate the K/Fe_3O_4/CNF from their media effectively is presented. This is evidenced by the low values of magnetic remanence (MR = 2.3(1) emu/g) and coercive field (HC = 6.2(1) mT), which has also previously been shown to be sufficient for limiting inter-particle magnetic interaction [38]. Meanwhile, the saturation magnetisation of M_S = 22.3(2) emu/g is comparable to other Fe_3O_4 based NPs, which undergo magnetic separation in solution by an applied external field [39].

3.2 Osmotic pressure analysis

DS osmotic pressure is the most essential property other than membrane properties that capacitate FO processes. It is the most critical condition that a functional material must fulfil relative to the feed stream for such material to function effectively as a draw agent in FO processes [2]. Fig. 7 represents the osmolality of varying concentrations of the K/Fe_3O_4/CNF

MNPs and that of 1.0 M NaCl solution, respectively. It can be seen that the osmolality of the samples is dependent on their various concentrations. Two different osmolality measurements were read for each sample concentration, and the average was computed as the final osmolality reading. The osmolality of the K/Fe_3O_4/CNF MNPs samples concentrations of 0.075 and 0.1 wt/vol% were 2112.5 and 3378 mOsmol/kg, which relates to 53.8 and 86.1 bar, respectively.

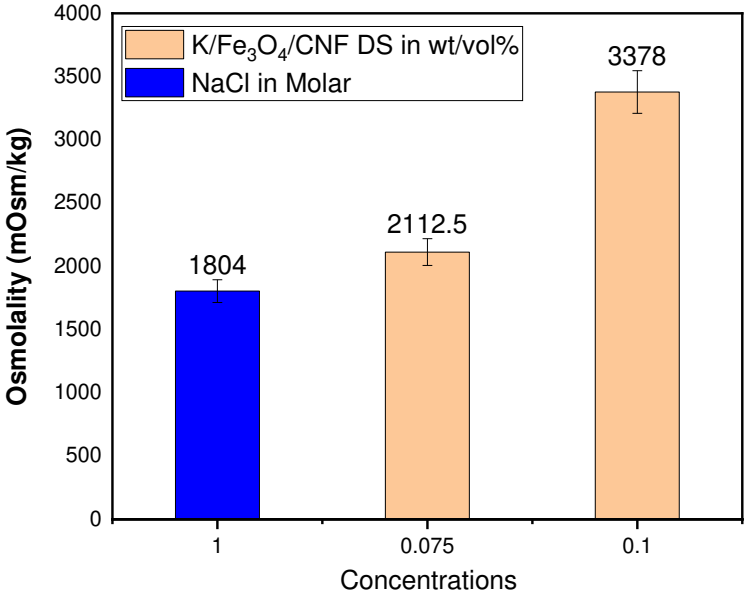

Fig. 7. The osmolality of K/Fe_3O_4/CNF DS at varying concentrations and 1.0 M NaCl solution.

Relatedly, the osmolality of 1.0 M NaCl solution was measured to be 1804 mOsmol/kg, corresponding to 45.96 bar. It is pertinent to note that the DS concentrations of 0.075 and 0.1 wt/vol% generated considerable osmotic pressures, respectively. This is in great contrast to other DS functional materials explored in other FO studies. For instance, a study by Dey et al. [40] could only register an osmotic pressure of ~11.37 atm (i.e. ~11.5 bar) with a DS concentration of 0.078 wt%. Different studies [15, 17-19, 26, 28, 41, 42] could only achieve some reasonable osmotic pressures at much higher DS concentrations between 0.35 - 74 wt% relative to the DS concentrations applied in this work. This indicates that the K/Fe_3O_4/CNF MNPs could generate even greater osmotic pressure and water flux with measured

concentrations higher than those utilised in this work. It further lends credence that the DS functional material in this study is potentially deployable in FO saltwater desalination on the strength of its osmotic pressures.

3.3 FO evaluation

The FO properties of K/Fe_3O_4/CNF DS were examined for different parameters, including osmotic pressure, water flux over time, average water flux, reverse salt flux, and specific reverse salt flux (SRSF) with the view to understanding its performance. Fig. 8(a) represents the cumulative permeate volume change over time. Incremental permeate volume change rose continuously, reflecting the volumetric weight loss in the feed tank containing the 1.0 M NaCl solution over time. Fig. 8(b, c and d) illustrates the water flux, reverse salt flux, and the change in electrical conductivity (feed tank) over time during the FO experiment with the K/Fe_3O_4/CNF DS. The water flux herein shown tend to be minimally impacted by the RSF, which is not unexpected considering obtained RSF value. The RSF exhibited some negative values at the initial stages, connoting bidirectional solutes diffusion. Negative ion flux highlights diffusion from the FS into the DS [43]. At high water flux, FS solutes move by advection to the membrane, at which point some may permeate through the membrane whilst the majority get rejected.

The result revealed a relatively stable water flux over the time of the FO experiment. As shown in Fig. 9, a cumulative water flux value of 37.8 LMH was attained when DI water was used as the FS at a DS concentration of 0.1 wt/vol%. On the other hand, 16.43 and 24 LMH water flux values were attained when 1 M NaCl solution was used as the FS at 0.075 and 0.1 wt/vol% DS concentrations, respectively. As opposed to the 1.0 M NaCl FS, where the FS might get concentrated over time as the DS become diluted, the DI water FS produced more water flux because the DS primarily confers the osmotic pressure gradient for the process without an

opposite or equal counteraction. Therefore, evaluating the osmotic activity of MNPs DS materials relative to saltwater conditions is more rational. So doing would further help to advance the potentialities of these MNPs DS materials in sure-enough conditions contrary to evaluating them versus DI water as the feed.

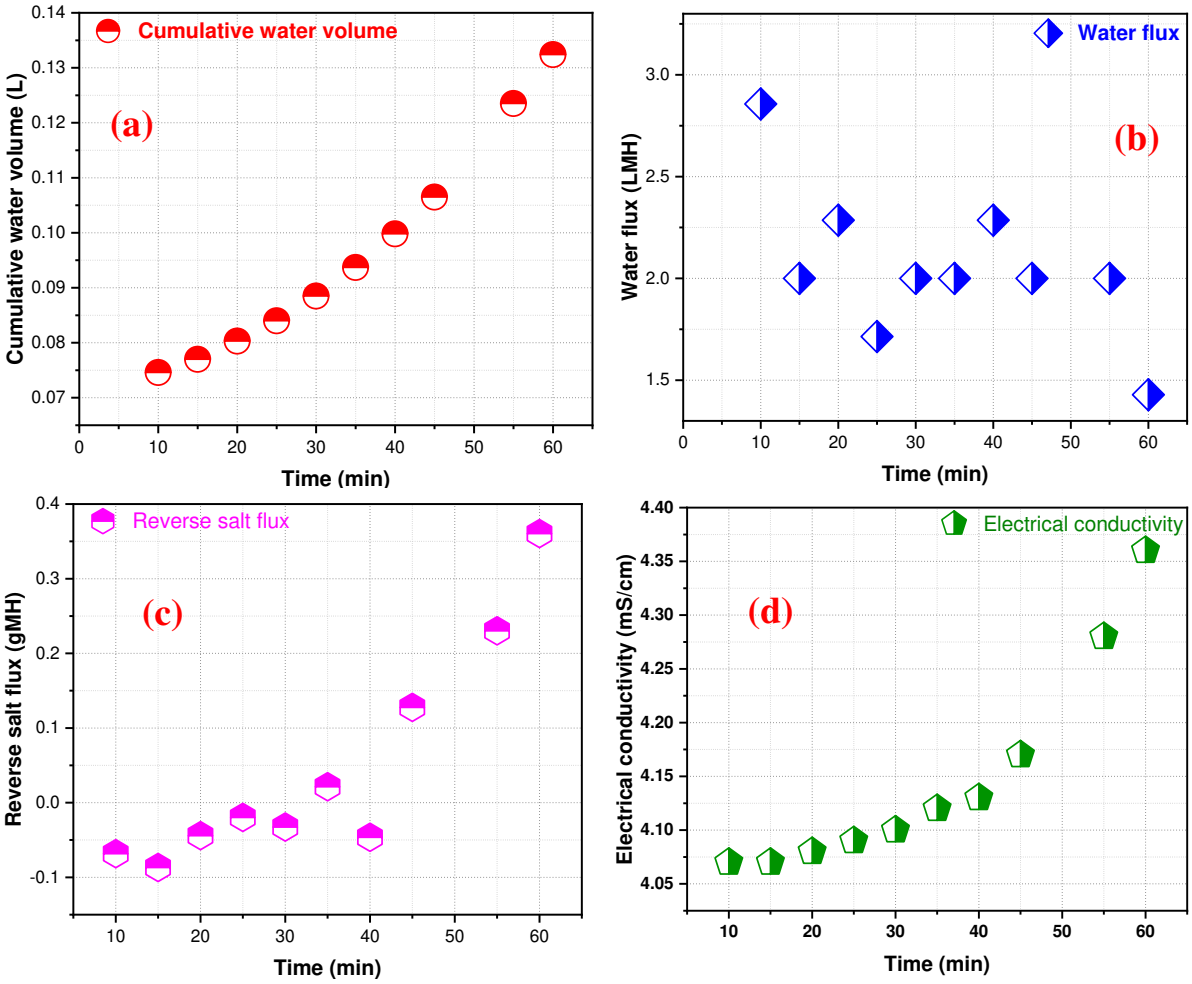

Fig. 8. a) Cumulative permeate volume over time; (b) water flux; (c) reverse salt flux (d); and electrical conductivity of the K/Fe_3O_4/CNF DS as a function of time.

The reason is that the ionic strength of feed streams, amongst other factors, can encumber water flux, especially in osmotic filtration processes where the membrane acts as the primary site of activities. Both results indicate a decrease in the water flux which can be attributed to different factors including a decrease in the osmotic driving force due to dilution of the DS [11, 27]. Other factors can be due to the inhibition of the pores of the membrane support layer because

of the large particles sizes of the DS material [27, 44]. This inference agrees with the trend of the water flux data in both cases. Particle size increases are known to adversely impact the osmotic driving force, which affects the overall FO system negatively [40]. At increased DS concentration and, by extension, the net osmotic pressure, the water flux increases. Such increases induce increased dilutive internal concentration polarization (ICP) inside the membrane support layer, reducing the overall driving force and water flux gains. Controlling the particle size of DS materials is, therefore, exigent. On the other hand, the hydrodynamic effects within the FO cell may have caused some NPs to abrade off the DS material whilst colliding with the membrane surface, depositing within the membrane pores in consequence [11, 27]. The deposition of the abraded NPs into the membrane pores is known to elicit severe ICP effects, constituting a limitation on the overall water flux [45]. As with MNPs, because they are not salts, the high energy potential NPs can migrate easily into the membrane pores, where they linger without necessarily exiting the pores [11], thereby constituting hindrance to the water flux. Modifying membranes with smart materials that have a high net surface charge to repel approaching particles might be plausible in mitigating particles' deposition into pores. The migrating NPs will bounce away from the membrane if the repulsive force is strong enough. Consequently, keeping them in a state of dispersion within the DS. In general, MNPs in colloids tend to aggregate if the interaction is permanent or agglomerate if their commingling is reversible [46]. These clustering mechanisms are known to have a significant negative impact on water flux, and may have played a role in this work. Although there are several methods of addressing issues related to agglomeration, surface modification of MNPs during material synthesis with suitable and sustainable modifiers like oleic acids should be given good consideration. It is noteworthy that whilst introducing hydrophilic groups via ligand exchange reactions helps improve surface hydrophilicity, their subsequent effect on defining size, modulating size distribution, and particles' effective magnetism requires careful consideration.

457 Because they can change some of the structural and magnetic properties of the modified MNPs,

458 limiting their efficiency and the system's overall performance.

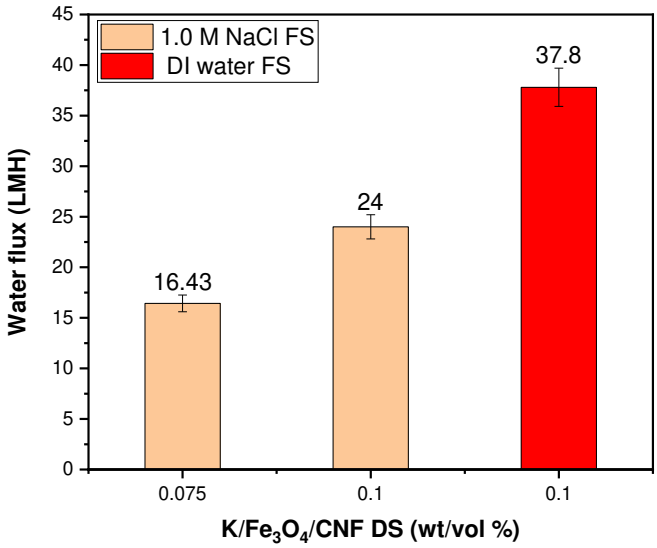

459

460 **Fig. 9**. Obtained water flux against varying concentrations of K/Fe_3O_4/CNF DS.

461

462 A glean from Table 1 shows that the K/Fe_3O_4/CNF performed remarkably well in water flux

463 relative to many of the DS, most of which were functionalised with hydrophilic polymer

464 compounds, and to which DI water was used as the feed in a good number of these studies. At

465 lower DS concentrations of 0.075 and 0.1 wt/vol%, respectively, the K/Fe_3O_4/CNF could

466 produce significant water flux (16.43 and 24 LMH) relative to what is achievable with a good

467 number of magnetic DS as reported in the literature at higher concentrations. Whilst

468 investigating MNPs as DS with DI water as the FS advances their potential application in FO

469 operations, it is critical to highlight that DI water as the FS does not exhibit osmotic resistance

470 to the MNPs DS as salt solutions do. Despite being tested against FS with high ionic strength

471 (1.0 M NaCl solution), the K/Fe_3O_4/CNF DS could advance water fluxes higher than those

472 achieved with existing MNPs as DS in previous studies utilising DI water as feed, which

473 provide no osmotic resistance to the DS.

474

475 **Table 1**. Comparison of water fluxes of different types of MNPs DS relative to varying DS

476 concentrations and source water feed streams.

Draw solutions	Concentration	Osmotic pressure	Initial water flux/time	Average water flux/time	Feed solution	Recovery process	References
PSSS-PNIPAM functionalized MNPs	33 wt%	55.0 (atm)	--	3.7 LMH and 2.7 LMH (1 h)	NaCl solution of 1000 mOsm/kg and 1200 mOsm/kg HTI membrane	Magnetic field & UF	[28]
Gelatin-coated MNPs	27g/L	1.50 (bar)	0.62 LMH (24 h)	--	0.01 M NaCl solution, HTI membrane	Magnetic field	[26]
Pectin coated MNPs	0.5 wt/vol%	--	6.6 LMH (120 min)	--	1.0 g% NaCl solution, Polyamide (PA) membrane	Magnetic field	[27]
Na/PAA MNPs	200 g/l	32.0 (atm)	2.0 LMH	--	Synthetic brackish water, HTI membrane	Electric field and NF	[15]
Poly-sodium-acrylate MNPs (PSA MNPs)	37 wt%	8.88 (atm)	4.3 LMH	--	DI water, CTA flat sheet membrane	Magnetic field and UF	[17]
SHPG-MNPs	400g/L	9.62 (atm)	3.0 LMH	--	DI water, CTA membrane	UF	[47]
Branched poly(deep eutectic solvent)-coated MNPs	3.5 g/l	68.0 (atm)	17.9 LMH (90 min)	--	DI water, CTA flat sheet membrane	Magnetic field	[19]
Poly(sodium acrylate) coated MNPs	0.078 wt%	11.37 (atm)	--	5.6 LMH (4 h)	DI water, Carbon nanotube membrane	Magnetic field	[40]
Citrate coated MNPs	20 mg/l	--	17.3 LMH (35 min)	--	DI water, CTA flat sheet membrane	Magnetic field	[11]

Sodium alginate sulfate MNPs	60 g/l	117.2 (atm)	--	8.6 LMH (60 min)	DI water, CTA flat sheet membrane	Magnetic field	[18]
K/Fe_3O_4/CNF	0.1 wt/vol% and 0.075 wt/vol%	86.1 (bar) 53.8 (bar)	24 LMH and 16.43 LMH (55 min)		1.0 M NaCl solution, CTA flat sheet membrane	Magnetic field	This work

To further probe the performance of the K/Fe_3O_4/CNF MNPs as a functional DS material, the RSF and SRSF of the DS material are examined. They are essential criteria when considering the suitability of a functional material as DS in FO processes [48]. The SRSF (J_s/J_w) helps with appraising the degree of draw solutes leakage into the feedstock per unit volume of water recovered across the membrane into the DS during FO processes [31, 48]. In contexts where high product quality is considered essential, SRSF value is particularly invaluable in designating the suitability of a functional DS material being deployed in such situations [42]. Because the 0.1 wt/vol% DS concentration exhibited much higher osmolality and, by extension, higher water flux, it was employed for elucidating RSF in this report. It can be observed that the RSF obtained during the experiment with the 0.1 wt/vol% DS concentration is ~ 0.56 gMH. Furthermore, an inappreciably small SRSF (ratio of J_s/J_w) value of 0.02 g/L is obtained from the maximum DS concentration in the sphere of this study.

Instructively, the degree of solute loss within the framework of this study appears to have fared reasonably well relative to that of varying ionic salts conventionally used as DS in FO operations, including MgCl, KCl, $Ca(NO_3)_2$, NaCl, NH_4Cl, CaCl, and NH_4HCO_3 as presented in Table 2. The SRSF value obtained in this work with the K/Fe_3O_4/CNF is negligible relative to SRSF values of the salts mentioned above in the range of ~0.57 – 2.48 g/L reported in previous studies [48]. The smaller SRSF value recorded in this work might not be unconnected to strong binding activity between the constituent nanoparticles of the functional DS material

during synthesis. Such strong binding between ions of the nanocomposite materials would likely have increased the diameter of the nanoparticles [28, 49] relative to the membrane pore sizes, which would have hindered the reverse diffusion of the draw solutes across the membrane into the feed stream. Such an insignificantly small SRSF value obtained in this work elicits the novel DS material's potential to be feasibly deployable in long-term operations in FO processes [31]. Nonetheless, because ions tend to permeate the membrane bidirectionally during FO operations, it will be well-advised to investigate how any diffusion of FS ions into the DS can modulate the DS's performance in future works.

Table 2. Reverse salt flux and specific reverse salt flux of commercial DS relative to K/Fe_3O_4/CNF DS

Draw solution	RSF (J_s) g/m^{2}h	SRSF (J_s/J_w) g/Lg/L	Reference
$MgCl_2$;	5.6	0.58	[48]
KCl	15.3	1.14	
$Ca(NO_3)_2$	6.6	0.62	
NaCl	9.1	0.75	
NH_4Cl	10.2	0.79	
CaCl	9.5	0.82	
NH_4HCO_3	18.2	2.48	
K/Fe_3O_4/CNF	0.56	0.02	This work

The DS preparation methodology deployed in this study eliminates the need for MNPs to be functionalised with hydrophilic polymers. In contrast to the TEG-K/CNF DS material fabricated in an earlier work by our group [31], the in-situ DS fabrication process employed in this work is facile, practical, and potentially more effective based on the obtained results. The polymer triethylene glycol (TEG) utilised in our previous work was replaced with Fe_3O_4. The new DS material could yet foster higher osmolality and higher water flux even at lower DS concentrations. The constituent materials utilised herein are biocompatible, non-toxic, and naturally occurring, which could be easily harnessed. Overall, this offers a potentially

517 sustainable methodology that can further bolster cost reductions applicable to FO desalination
518 processes. Ordinarily, the colloidal solutions of Fe_3O_4 MNPs are understood to exhibit
519 inappreciable osmotic pressure even at higher concentrations [50], and this is the same case
520 with CNF. However, it follows that incorporating K-species in the synthesis and some
521 hydrophilic ligands absorbed into the surfaces of the Fe_3O_4 and CNF generated osmotic
522 pressure build-up within the DS nano-fluid. Consequently, the enhanced osmotic effect
523 facilitated by the K-species and the hydrophilic groups in the DS ensured a sustained osmotic
524 diffusion of water molecules across the CTA membrane from the feed stream over time.
525

526 **4. Conclusions**

527 The potential application of K/Fe_3O_4/CNF MNPs as a novel DS in FO desalination was
528 successfully demonstrated. The DS preparation protocol established in this study is
529 advantageous as it is eco-friendly, and it eliminates the often recourse to polymer compounds
530 for the needed hydrophilic functionality in MNPs. Yet, the K/Fe_3O_4/CNF attained enhanced
531 hydrophilicity. Moreover, the facile DS synthesis strategy will potentially open a new route to
532 preparing other DS nanomaterials with unique multi functionalities and enhanced
533 hydrophilicity without recourse to polymers. The novel draw solution generated considerable
534 osmotic pressure of 86.1 bar, high enough to desalinate highly saline feed streams. It also
535 occasioned a high cumulative water flux of 24 LMH at a DS concentration of 0.1 wt/vol%
536 utilising a CTA membrane. Draw solutes eliciting higher water flux at lower DS concentrations
537 will be preferable, considering that they can contribute to considerable reductions in the overall
538 capital expenditures in FO operations. Relative to several organic and inorganic salts in
539 literature commercially used as DS in FO operations, negligibly low reverse salt flux and
540 specific reverse salt flux values of ~ 0.56 gMH and ~ 0.02 g/L were recorded with the novel
541 DS. However, to offset the negative impact of bigger particle sizes on water flux, it is necessary

to carefully manage the particle size distribution of DS materials during synthesis, notwithstanding its positive influence on RSF. Furthermore, it will be well-thought for future research to fully appraise the energy implication and the overall economic merit of magnetic field DS reconcentration and water recovery relative to other DS recovery methods. This is considering the often requirement of ultrafiltration with magnetic separation in contexts where high product water quality is required as the final product. Although the predisposition of membrane fouling with the K/Fe_3O_4/CNF DS is not investigated in this work, it is pertinent to explore this in future studies to ascertain the extent to which fouling may or otherwise impact water flux in utilising this novel DS material. In the next phase of this study, our group will consider the FO system integrating magnetic field and solar-thermal separability to attempt the feasibility of solute recovery of smaller sized MNPs.

Acknowledgements

We acknowledge the technical support provided by Dr Adrian Cunliffe, Ms Karine Alves Thorne and Dr Ben Douglas for access to the analytical equipment, Mr Stuart Micklethwaite for performing SEM images, and Mr Mohammed Javed for collecting XRD data. D.H. acknowledges financial support from the Engineering and Physical Sciences Research Council (EP/S032797/1). A.A. thanks the Petroleum Technology Development Fund (PTDF) in Nigeria (PTDF/AAJ/250/17) for funding.

CRediT authorship contribution statement:

Aondohemba Aende: Performed the FO experiments, characterisations of DS, formal analysis, funding, and drafted the first version of the manuscript. Jabbar Gardy: Originated idea, synthesised the draw solution, methodology, provided support with DS characterisations, investigation, supervised the work, and writing - review & editing; Zabeada Aslam: Collected

data on Titan TEM and provided supports in TEM analysis, investigation, and writing - review & editing; Matthew Rogers: Collected data on SQUID and provided support with magnetism analysis, investigation, and writing - review & editing; Mohamed Edokali: Provided supports with FO experiments and analysis, investigation, writing - review & editing, Oscar Cespedes: Provided support with magnetism analysis, investigation, and writing - review & editing; David Harbottle: Supervised the work, funding, investigation, and writing - review & editing; Ali Hassanpour: Provided supports with FO data analysis, supervised the work, investigation, project management, and writing - review & editing.

Corresponding authors info:

1- Associate Prof Ali Hassanpour − School of Chemical and Process Engineering, University of Leeds, Leeds LS2 9JT, U.K.; https://orcid.org/0000-0002-7756-1506; Phone: +44(0)1133432405; Email: A.Hassanpour@leeds.ac.uk

2- Dr Jabbar Gardy − School of Chemical and Process Engineering, University of Leeds, Leeds LS2 9JT, U.K.; https://orcid.org/0000-0003-1806-4056; Phone: +44(0)7392333760; Email: J.Gardy@leeds.ac.uk

References

1. Shatat, M., Riffat, Saffa B., *Water desalination technologies utilizing conventional and renewable energy sources.* International Journal of Low-Carbon Technologies, 2012. **9**(1): p. 1-19.
2. Aende, A., Gardy, Jabbar, Hassanpour, Ali, *Seawater desalination: A review of forward osmosis technique, its challenges, and future prospects.* Processes, 2020. **8**(8): p. 901.
3. World-Bank *The role of desalination in an increasingly water-scarce world*. 2019.
4. Programme), W.-U.N.W.W.A., *The United Nations World Water Development Report 2014: Water and Energy*. 2014, UNESCO: Paris.
5. Bell, E.A., Holloway, Ryan W., Cath, Tzahi Y., *Evaluation of forward osmosis membrane performance and fouling during long-term osmotic membrane bioreactor study.* Journal of Membrane Science, 2016. **517**: p. 1-13.
6. McCutcheon, J.R., McGinnis, Robert L., Elimelech, Menachem, *A novel ammonia—carbon dioxide forward (direct) osmosis desalination process.* Desalination, 2005. **174**(1): p. 1-11.

7. Martinetti, C., Childress, A., Cath, T., *High recovery of concentrated RO brines using forward osmosis and membrane distillation.* Journal of Membrane Science, 2009. **331**: p. 31-39.
8. Shaffer, D.L.W., Jay R. Jaramillo, Humberto Lin, Shihong Elimelech, Menachem, *Forward osmosis: Where are we now?* Desalination, 2015. **356**: p. 271-284.
9. Chekli, L.P., Sherub Kim, Jung Eun Kim, Jihye Choi, Joon Young Choi, June-Seok Kim, Suhan Kim, Joon HaHong, Seungkwan Sohn, Jinsik Shon, H. K., *A comprehensive review of hybrid forward osmosis systems: Performance, applications and future prospects.* Journal of Membrane Science, 2016. **497**: p. 430-449.
10. Hafiz, M., et al., *Optimization of Magnetic Nanoparticles Draw Solution for High Water Flux in Forward Osmosis.* Water, 2021. **13**(24).
11. Na, Y., Yang, Seungheon, Lee, Seockheon, *Evaluation of citrate-coated magnetic nanoparticles as draw solute for forward osmosis.* Desalination, 2014. **347**: p. 34-42.
12. Kharisov, B.I.D., H. V. Rasika Kharissova, Oxana V. Vázquez, Alejandro Peña, Yolanda Gómez, Idalia, *Solubilization, dispersion and stabilization of magnetic nanoparticles in water and non-aqueous solvents: recent trends.* RSC Advances, 2014. **4**(85): p. 45354-45381.
13. Ge, Q.S., Jincai Chung, Tai-Shung Amy, Gary, *Hydrophilic superparamagnetic nanoparticles: Synthesis, characterization, and performance in forward osmosis processes.* Industrial & Engineering Chemistry Research, 2011. **50**(1): p. 382-388.
14. Bai, H., Liu, Zhaoyang, Sun, Darren Delai, *Highly water soluble and recovered dextran coated Fe_3O_4 magnetic nanoparticles for brackish water desalination.* Separation and Purification Technology, 2011. **81**(3): p. 392-399.
15. Ling, M.M., Chung, Tai-Shung, *Surface-dissociated nanoparticle draw solutions in forward osmosis and the regeneration in an integrated electric field and nanofiltration system.* Industrial & Engineering Chemistry Research, 2012. **51**(47): p. 15463-15471.
16. Mokhtar Guizani, T.M., Ryusei Ito, Naoyuki Funamizu, *Engineering of size-controlled magnetic nanoparticles for use as a draw solution in a forward osmosis process.* Desalination and Water Treatment, 2019. **154**: p. 9.
17. Ban, I., Markuš, Sabina, Gyergyek, Sašo, Drofenik, Miha, Korenak, Jasmina, Helix-Nielsen, Claus, Petrinić, Irena, *Synthesis of poly-sodium-acrylate (PSA)-coated magnetic nanoparticles for use in forward osmosis draw solutions.* Nanomaterials, 2019. **9**(9): p. 1238.
18. Khazaie, F., Shokrollahzadeh, Soheila, Bide, Yasamin, Sheshmani, Shabnam, Shahvelayati, Ashraf S., *Forward osmosis using highly water dispersible sodium alginate sulfate coated-Fe_3O_4 nanoparticles as innovative draw solution for water desalination.* Process Safety and Environmental Protection, 2021. **146**: p. 789-799.
19. Bide, Y., Shokrollahzadeh, Soheila, *Toward tailoring of a new draw solute for forward osmosis process: Branched poly (deep eutectic solvent)-decorated magnetic nanoparticles.* Journal of Molecular Liquids, 2020. **320**: p. 114409.
20. Zhou, A., Luo, Huayong, Wang, Qin, Chen, Lin, Zhang, Tian C., Tao, Tao, *Magnetic thermoresponsive ionic nanogels as novel draw agents in forward osmosis.* RSC Advances, 2015. **5**(20): p. 15359-15365.
21. Ling, M.M., Chung, Tai-Shung, Lu, Xianmao, *Facile synthesis of thermosensitive magnetic nanoparticles as "smart" draw solutes in forward osmosis.* Chemical Communications, 2011. **47**(38): p. 10788-10790.
22. Moeser, G., et al., *High-gradient magnetic separation of coated magnetic nanoparticles.* AIChE Journal, 2004. **50**: p. 2835-2848.

23. Ling, M.M. and T.-S. Chung, *Desalination process using super hydrophilic nanoparticles via forward osmosis integrated with ultrafiltration regeneration.* Desalination, 2011. **278**(1): p. 194-202.
24. Mazlan, N.M., D. Peshev, and A.G. Livingston, *Energy consumption for desalination — A comparison of forward osmosis with reverse osmosis, and the potential for perfect membranes.* Desalination, 2016. **377**: p. 138-151.
25. Ling, M.M., Chung, Tai-Shung, *Desalination process using super hydrophilic nanoparticles via forward osmosis integrated with ultrafiltration regeneration.* Desalination, 2011. **278**(1): p. 194-202.
26. Azadi, F., Karimi-Jashni, Ayoub, Zerafat, Mohammad Mahdi, *Desalination of brackish water by gelatin-coated magnetite nanoparticles as a novel draw solute in forward osmosis process.* Environmental Technology, 2021. **42**(18): p. 2885-2895.
27. Tayel, A., Nasr, Peter, Sewilam, H., *Forward osmosis desalination using pectin-coated magnetic nanoparticles as a draw solution.* Clean Technologies and Environmental Policy, 2019. **21**: p. 1617 - 1628.
28. Zhao, Q., Chen, Ningping, Zhao, Dieling, Lu, Xianmao, *Thermoresponsive magnetic nanoparticles for seawater desalination.* ACS Applied Materials & Interfaces, 2013. **5**(21): p. 11453-11461.
29. Gardy, J., Nourafkan, Ehsan, Osatiashtiani, Amin, Lee, Adam F., Wilson, Karen, Hassanpour, Ali, Lai, Xiaojun, *A core-shell SO_4/Mg-Al-Fe_3O_4 catalyst for biodiesel production.* Applied Catalysis B: Environmental, 2019. **259**: p. 118093.
30. Fipps, G. *Irrigation water quality standards and salinity management strategies*. 30-04-2003.
31. Amjad, M., Gardy, Jabbar, Hassanpour, Ali, Wen, Dongsheng, *Novel draw solution for forward osmosis based solar desalination.* Applied Energy, 2018. **230**: p. 220-231.
32. Nandiyanto, A., Oktiani, Rosi, Ragadhita, Risti, *How to read and interpret FTIR spectroscope of organic material.* Indonesian Journal of Science and Technology, 2019. **4**: p. 97-118.
33. Suzuki, A., Kebukawa, Yoko, Nakashima, Satoru, Keller, Lindsay, Zolensky, M., Nakamura, T., *Infrared micro-spectroscopy of organic and hydrous components in some antarctic micrometeorites.* 2005.
34. Donald L. Pavia, G.M.L., George S. Kriz, and James R. Vyvyan, *Introduction to spectroscopy*, M. Limited, Editor. 2015, Cengage Learning: United States of America. p. 786.
35. Zhou, J.-H., Sui, Zhi-Jun, Zhu, Jun, Li, Ping, Chen, De, Dai, Ying-Chun, Yuan, Wei-Kang, *Characterization of surface oxygen complexes on carbon nanofibers by TPD, XPS and FT-IR.* Carbon, 2007. **45**(4): p. 785-796.
36. Park, S.K., Sure, Jagadeesh, Vishnu, D. S., Jo, Seong J., Lee, Woo C., Ahmad, Ibrahim A., Kim, Hyun-Kyung, *Nano-Fe_3O_4/carbon nanotubes composites by one-pot microwave solvothermal method for supercapacitor applications.* Energies, 2021. **14**(10).
37. Hesas, R.H., Baei, Mazyar Sharifzadeh, Rostami, Hadi, Gardy, Jabbar, Hassanpour, Ali, *An investigation on the capability of magnetically separable Fe_3O_4/mordenite zeolite for refinery oily wastewater purification.* Journal of Environmental Management, 2019. **241**: p. 525-534.
38. Gardy, J., Osatiashtiani, Amin, Céspedes, Oscar, Hassanpour, Ali, Lai, Xiaojun, Lee, Adam F., Wilson, Karen, Rehan, Mohammad, *A magnetically separable SO_4/Fe-Al-TiO_2 solid acid catalyst for biodiesel production from waste cooking oil.* Applied Catalysis B: Environmental, 2018. **234**: p. 268-278.
39. Moghanian, H., Mobinikhaledi, A., Blackman, A. G., Sarough-Farahani, E., *Sulfanilic acid-functionalized silica-coated magnetite nanoparticles as an efficient, reusable and*

magnetically separable catalyst for the solvent-free synthesis of 1-amido- and 1-aminoalkyl-2-naphthols. RSC Advances, 2014. **4**(54): p. 28176-28185.

40. Dey, P., Izake, Emad L., *Magnetic nanoparticles boosting the osmotic efficiency of a polymeric FO draw agent: Effect of polymer conformation.* Desalination, 2015. **373**: p. 79-85.
41. Park, S.Y., Ahn, Hyo-Won, Chung, Jae Woo, Kwak, Seung-Yeop, *Magnetic core-hydrophilic shell nanosphere as stability-enhanced draw solute for forward osmosis (FO) application.* Desalination, 2016. **397**: p. 22-29.
42. Ge, Q., Su, Jincai, Amy, Gary L., Chung, Tai-Shung, *Exploration of polyelectrolytes as draw solutes in forward osmosis processes.* Water Research, 2012. **46**(4): p. 1318-1326.
43. Coday, B.D., et al., *Effects of Transmembrane Hydraulic Pressure on Performance of Forward Osmosis Membranes.* Environmental Science & Technology, 2013. **47**(5): p. 2386-2393.
44. Cannon, J., et al., *Influence of Ion Size and Charge on Osmosis.* The Journal of Physical Chemistry B, 2012. **116**(14): p. 4206-4211.
45. Phillip, W.A., J.S. Yong, and M. Elimelech, *Reverse Draw Solute Permeation in Forward Osmosis: Modeling and Experiments.* Environmental Science & Technology, 2010. **44**(13): p. 5170-5176.
46. Gutiérrez, L., et al., *Aggregation effects on the magnetic properties of iron oxide colloids.* Nanotechnology, 2019. **30**(11): p. 112001.
47. Yang, H.-M., Choi, Hye, Jang, Sung-Chan, Han, Myeong-Jin, Seo, Bum-Kyoung, Moon, Jei-Kwon, Lee, Kune-Woo, *Succinate functionalization of hyperbranched polyglycerol-coated magnetic nanoparticles as a draw solute during forward osmosis.* Journal of Nanoscience and Nanotechnology, 2015. **15**.
48. Achilli, A., Cath, Tzahi Y., Childress, Amy E., *Selection of inorganic-based draw solutions for forward osmosis applications.* Journal of Membrane Science, 2010. **364**(1): p. 233-241.
49. Yang, Q., Lei, Jing, Sun, Darren D., Chen, Dong, *Forward osmosis membranes for water reclamation.* Separation & Purification Reviews, 2016. **45**(2): p. 93-107.
50. Ban, I., Markuš, S., Gyergyek, S., Drofenik, M., Korenak, J., Helix-Nielsen, C., Petrinić, I., *Synthesis of poly-sodium-acrylate (PSA)-coated magnetic nanoparticles for use in forward osmosis draw solutions.* Nanomaterials (Basel), 2019. **9**(9).